# Influence of Ocean Currents on Wave Modeling and Satellite Observations Insights From the One Ocean Expedition

Altiparmaki, Ourania; Breivik, Øyvind; Aouf, Lotfi; Bohlinger, Patrik; Johannessen, Johnny A.; Collard, Fabrice; Donlon, Craig; Hope, Gaute; Visser, Pieter N.A.M.; Naeije, Marc

**DOI**
10.1029/2024JC021581

**Publication date**
2024

**Document Version**
Final published version

**Published in**
Journal of Geophysical Research: Oceans

**Citation (APA)**
Altiparmaki, O., Breivik, Ø., Aouf, L., Bohlinger, P., Johannessen, J. A., Collard, F., Donlon, C., Hope, G., Visser, P. N. A. M., & Naeije, M. (2024). Influence of Ocean Currents on Wave Modeling and Satellite Observations: Insights From the One Ocean Expedition. *Journal of Geophysical Research: Oceans*, *129*(11), Article e2024JC021581. https://doi.org/10.1029/2024JC021581

JGR Oceans

RESEARCH ARTICLE
10.1029/2024JC021581

# Influence of Ocean Currents on Wave Modeling and Satellite Observations: Insights From the One Ocean Expedition

**Ourania Altiparmaki[1], Øyvind Breivik[2,3], Lotfi Aouf[4], Patrik Bohlinger[2], Johnny A. Johannessen[5], Fabrice Collard[6], Craig Donlon[7], Gaute Hope[2], Pieter N. A. M. Visser[1], and Marc Naeije[1]**

[1]Astrodynamics and Space Missions, Aerospace Engineering, Delft University of Technology, Delft, The Netherlands, [2]Norwegian Meteorological Institute, Bergen, Norway, [3]Geophysical Institute, University of Bergen, Bergen, Norway, [4]Météo-France, DIROP-CNRM, Toulouse, France, [5]Nansen Environmental and Remote Sensing Center, Bergen, Norway, [6]OceanDataLab, Brest, France, [7]ESTEC ESA, Noordwijk, The Netherlands

**Abstract** This study investigates the influence of ocean currents on wave modeling and satellite observations using in situ wave measurements from the One Ocean Expedition 2021–2023. In January 2023, six OpenMetBuoy drifters were deployed in the Agulhas Current region. Their high immersion ratio minimized wind effects, allowing them to follow the current and return to the Indian Ocean by the Agulhas retroflection, collecting data for about 2 months. Comparing surface current velocities from both the Mercator model and Globcurrent product with drifter data reveals underestimation for velocities over 0.5 m $s^{-1}$ with Mercator showing greater variability. Significant wave height and Stokes drift parameters from MFWAM and ERA5 were also evaluated against drifters. Both models tend to overestimate Stokes drift more noticeable in ERA5, indicating sensitivity to wind seas. For significant wave height, both models agree well with drifter measurements with correlations of 0.90 for MFWAM and 0.83 for ERA5. However, ERA5's lack of surface current data combined with its coarse resolution (0.5°) lead to underestimation of wave heights exceeding 2.5 m. MFWAM products including and excluding currents exhibit root mean square errors of 0.39 and 0.45 m, respectively, when compared to drifter measurements. This confirms that neglecting currents introduces additional errors particularly in areas with sharp current gradients. Analyzing MFWAM wave spectra, including and excluding currents, reveals wave energy transfer attributed to wave-current interactions. The spatial extent of these interactions is captured by satellite altimeters, revealing wave modulations with considerable wave height variations when waves cross eddies and the current core.

**Plain Language Summary** Our study explores how ocean waves interact with surface currents in the Agulhas Current region, an important western boundary current of the global ocean circulation, reaching velocities up to 3 m $s^{-1}$. In 2023, we deployed six drifters with the goal to assess the performance of wave models and satellite observations in this dynamic environment. We found that two commonly used ocean current products, Mercator and Globcurrent, often underestimate current speeds above 0.5 m $s^{-1}$ compared to the drifters. We also evaluated wave height predictions from two models: the Météo-France Wave Model (MFWAM), which considers surface currents, and the European Center for Medium-Range Weather Forecasts Reanalysis v5 (ERA5), which does not. Our results showed that ERA5 often underestimates waves higher than 2.5 m, indicating that not accurately modeling ocean conditions can lead to significant errors. Wave height comparisons between drifters and satellite altimeters revealed good agreement. Additionally, using satellite data, we showcased how currents affect wave heights, especially around swirling waters (eddies) and when waves cross the current. Overall, our research highlights the need for more work in the area of wave-current interactions and the importance of including these processes in wave modeling using multisource data.

**Key Points:**

- Drifters show Mercator and Globcurrent underestimate current speeds, a trend increasing with stronger currents and higher sea states
- Neglecting current data in wave modeling leads to significant underestimation of wave heights
- Satellite altimetry data reveal wave height modulations around the Agulhas Current, indicating signatures of wave-current interactions

**Correspondence to:**
O. Altiparmaki,
O.Altiparmaki@tudelft.nl

**Citation:**
Altiparmaki, O., Breivik, Ø., Aouf, L., Bohlinger, P., Johannessen, J. A., Collard, F., et al. (2024). Influence of ocean currents on wave modeling and satellite observations: Insights from the one ocean expedition. *Journal of Geophysical Research: Oceans*, *129*, e2024JC021581. https://doi.org/10.1029/2024JC021581

Received 13 JUL 2024
Accepted 18 OCT 2024

**Author Contributions:**
**Conceptualization:** Ourania Altiparmaki, Øyvind Breivik, Lotfi Aouf
**Data curation:** Ourania Altiparmaki, Lotfi Aouf, Patrik Bohlinger, Gaute Hope, Marc Naeije
**Formal analysis:** Ourania Altiparmaki
**Funding acquisition:** Johnny A. Johannessen, Craig Donlon, Pieter N. A. M. Visser, Marc Naeije
**Investigation:** Ourania Altiparmaki
**Methodology:** Ourania Altiparmaki, Øyvind Breivik
**Project administration:** Pieter N. A. M. Visser, Marc Naeije
**Resources:** Øyvind Breivik, Fabrice Collard
**Software:** Ourania Altiparmaki, Patrik Bohlinger
**Supervision:** Øyvind Breivik, Lotfi Aouf, Patrik Bohlinger, Pieter N. A. M. Visser, Marc Naeije
**Validation:** Ourania Altiparmaki



## 1. Introduction

Understanding the complex interactions between ocean waves and currents is essential for accurate wave forecasts as they significantly affect wave dynamics and energy distribution. Ocean currents, influenced by factors such as wind variations, temperature, and salinity gradients, possess the ability to alter wave characteristics, including their amplitude and direction. This phenomenon, known as refraction, instigates energy transfer between currents and waves (Holthuijsen, 2007), often leading to the steepening of waves and the emergence of abnormal sea states characterized by extreme wave heights (Barnes & Rautenbach, 2020; Ponce de León &

**Visualization:** Ourania Altiparmaki
**Writing – original draft:** Ourania Altiparmaki
**Writing – review & editing:** Ourania Altiparmaki, Øyvind Breivik, Lotfi Aouf, Patrik Bohlinger, Johnny A. Johannessen, Fabrice Collard, Craig Donlon, Gaute Hope, Pieter N. A. M. Visser, Marc Naeije

Guedes Soares, 2021; Quilfen et al., 2018). Such conditions can pose significant hazards to maritime activities and are critical for search and rescue operations, emphasizing the need for high-quality wave forecasts in current dominated regions to ensure safety. Additionally, surface currents affect air-sea interactions, including the fluxes of heat, carbon dioxide, and momentum. They also impact coastal ecosystems, making it essential to monitor their strength and variability to understand environmental changes and ensure accurate climate predictions.

In recent decades, satellite remote sensing instruments have radically changed the study of ocean waves and currents on a global scale. Satellite altimetry allows the estimation of detailed maps of geostrophic currents (Rio et al., 2014), while offering consistent measurements of significant wave height and stress-equivalent wind speed globally (Hayne, 1980; Raney, 1998). Synthetic aperture radar (SAR) altimetry has shown promise in retrieving swell wave spectra (Altiparmaki et al., 2022; Kleinherenbrink et al., 2024), whereas satellites such as Sentinel-1 and CFOSAT contribute significantly to global wave spectra products (Ren et al., 2017; Torres et al., 2012). Studies leveraging these advances have provided insights into how surface currents deflect incoming swell waves, resulting in phenomena such as wave trapping (Irvine & Tilley, 1988; Krug et al., 2010; Kudryavtsev et al., 2017; Marghany, 2018; Quilfen & Chapron, 2019). Despite these advances, accurately quantifying wave-current interaction effects at regional scales requires high-resolution and multispectral observations. However, challenges, such as data continuity, spatial resolution, and coverage limitations, persist.

Wave models are essential for short-term forecasting (5–10 days) but often fail to capture the complex interplay between waves and currents, particularly when high-quality current data are lacking or currents are entirely neglected. Notably, neglecting currents in the simulations significantly affects wave height predictions, highlighting the need for surface current forcing to prevent major discrepancies especially in regions prone to developing extreme waves (Ponce de León & Guedes Soares, 2021). Once current forcing is considered, several factors contribute to the complexity of accurately modeling its impact on waves. Some of them are related to the complex ocean dynamics in coastal zones, where bathymetry, coastline geometry, wave breaking, and tidal variations complicate wave-current interactions (Komijani & Monbaliu, 2019). These factors significantly influence the evolution of the wave field, intensifying the nonlinear interactions between waves and currents (Pascolo et al., 2018). Moreover, the spatial and temporal resolution of wave models may fail to capture the rapid variability of currents (Ponce de León & Guedes Soares, 2021), underlining the ongoing need to improve these models through data assimilation methods and validation activities against in situ measurements.

Undoubtedly, in situ measurements from moored buoys, drifters, and research vessels provide highly accurate data. However, collecting such measurements over large spatial scales is challenging due to high maintenance costs and maritime conditions. Consequently, relying solely on these data limits our understanding of the broader impacts of currents on waves, which extend beyond local ocean processes. For instance, swell waves interacting with strong currents can undergo refraction kilometers away from their initial point of interaction, complicating the monitoring of their evolution (Halsne et al., 2023).

The consideration of various data sources, including in situ measurements and satellite observations, enhances our ability to better understand complex dynamics of ocean circulation and achieve reliable predictions, thereby contributing to more accurate climate models and effective marine resource management. Our study exploits in situ measurements from drifters deployed during the ESA-PECO2 Advanced Ocean Training Course 2023, part of the One Ocean Expedition 2021–2023, in the Agulhas Current region to evaluate the current impact on wave models and satellite observations (https://oneoceanexpedition.com/). The Agulhas Current is considered one of the world's strongest western boundary currents with surface velocities exceeding 3 m $s^{-1}$ (Lutjeharms, 2007; Naeije et al., 1992). This feature makes its study essential for understanding the climate system and marine biodiversity of the Indian Ocean. Moreover, its strength and dynamic mesoscale structures provide a unique natural laboratory for studying wave-current interactions.

The article is structured as follows. Section 2 details the methods and data acquisition process, including in situ measurements, satellites, and wave models. Section 3 presents comparative analyses of drifter-derived surface current speed, significant wave height, and surface Stokes drift against wave models and satellite products. Initially, we examine surface current speeds as estimated by the drifters, the altimetry-derived Globcurrent product and the Mercator model. Subsequently, we perform a similar analysis on the impact of currents on significant wave height and Stokes drift products of the European Center for Medium-Range Weather Forecasts Reanalysis v5 (ERA5) and Copernicus Marine Environment Monitoring Service Météo-France WAve Model

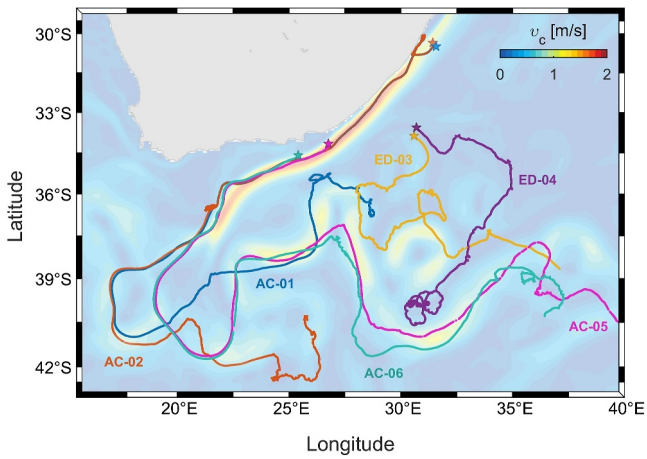


**Figure 1.** Mean Mercator surface current velocities ($v_c$ is plotted in the background using inserted color scale) and drifters' trajectories from 05-January-2023 to 28-February-2023: Four drifters were deployed in the Agulhas core (AC) and two in the vicinity of eddies (ED). The star-shaped markers indicate the deployment locations.

(MFWAM). Section 4 extends this analysis by utilizing customized MFWAM wave spectra, computed both with and without current forcing, highlighting the importance of including surface current data in wave modeling. Section 5 focuses on the contribution of satellite altimetry in identifying wave-current interactions, emphasizing the critical role of multisource data in understanding current-induced wave modulations. The article concludes in Section 6 with a summary of the key findings.

## 2. Data and Methods

### 2.1. OpenMetBuoy Drifters

During the One Ocean Expedition 2021–2023, six OpenMetBuoy drifters were deployed in the Agulhas Current region as part of the ESA-PECO2 Advanced Ocean Training Course 2023 held aboard the Statsraad Lehmkuhl sailing ship. The drifters, named OpenMetBuoy (Rabault et al., 2022), have lateral dimensions of 16 × 16 cm and a height of 9 cm with approximately 3 cm of overwater structure. Powered by alkaline batteries, these drifters had an operational period of approximately 2 months, which could be extended with higher-capacity batteries. Each drifter was equipped with an inertial measurement unit (IMU) with six degrees of freedom, enabling precise high-frequency measurements of acceleration and angular rates in the three spatial dimensions. Wave spectra, covering a frequency range between 0.040 and 0.307 Hz, were acquired at fixed intervals with measurements taken for 20 min every 3 hr. Additionally, a GPS module was integrated for tracking the drifters' positions every 30 min. Over the 2-month data collection period, the drifters' trajectories revealed distinct movement patterns. Figure 1 depicts these paths, plotted over mean surface current velocities obtained from the Copernicus Mercator product.

Four of the drifters were deployed within the core of the Agulhas Current, following the current toward the retroflection area and then toward the Indian Ocean. In particular, AC-01 and AC-02 were initially deployed together but drifted apart around the retroflection area. AC-05 and AC-06 were deployed approximately 12 hr apart with an initial separation of over 200 km yet remained relatively close to each other until their power supplies were depleted. The remaining two drifters, ED-03 and ED-04, were deployed with a separation of about 30 km in the anticyclonic and cyclonic part of a vortex pair southeast of the Agulhas Current and quickly diverged from each other. Notably, both drifters exhibited inertial oscillations over periods of days likely induced by sudden changes in local winds (Pollard, 1980).

The observed patterns clearly show that the drifters closely followed the surface currents. Their small size and immersion-to-windage ratio minimized the impact of direct windage effects, which proved especially advantageous in the Agulhas Current where surface drift is primarily driven by geostrophic currents (Lutjeharms, 2007). As a result, we were able to infer the surface current directly from the drifter trajectories,

$$v_{\mathrm{dr}} \approx \frac{\Delta s}{\Delta t}. \tag{1}$$

Here, $\Delta t$ represents a 30-min time interval and $\Delta s$ the distance traveled by a drifter during this period. An outlier removal scheme is implemented in two steps. First, outliers are rejected, setting a threshold for records taken at time intervals of less than 30 min. Second, records acquired with a time interval exceeding 3 hr were deemed to be of poor quality and subsequently excluded from the analysis. Then, considering linear wave theory, the significant wave height and the Stokes drift velocity are calculated from the ocean wave spectrum $F()$,

$$H_s = 4\sqrt{\int_0^{\infty} F(\omega)d\omega} \tag{2}$$

**Table 1**
*List of the Parameters and Setup Used as the Forcing Conditions for Both Satellite and Wave Model Products*

| | Mercator | Globcurrent (NRT) | ERA5 | MFWAM |
|---|---|---|---|---|
| Spatial resolution | 1/12° | 1/4° | 1/2° | 1/12° |
| Temporal resolution (h) | 6 | 1 | 1 | 3 |
| Wind speed | N/A | Global Ocean[a] | ERA5 | IFS-ECMWF |
| Bathymetry | ETOPO1 | ETOPO1 | ETOPO2 | ETOPO2 |
| Current forcing | N/A | N/A | NO | (a) Mercator PSY4 (daily)<br>(b) Globcurrent (daily)<br>(c) NO |

[a]Copernicus Product ID:WIND_GLO_PHY_L4_NRT_012_004.

$$v_{\mathrm{st,dr}}(z) = \frac{2}{g}\int_0^{2\pi}\int_0^{\infty} \omega^3 \hat{\mathbf{k}} e^{2kz} F(\omega,\theta)\, d\omega\, d\theta. \tag{3}$$

Here, $\theta$ denotes the direction in which the wave component is traveling, $\omega = 2\pi f$ is the circular frequency with $f$ the linear frequency and $\hat{\mathbf{k}}$ the unit vector in the direction of wave propagation (Kenyon, 1969). For the purpose of our study, depth, denoted by $z$, is set to zero as we are solely interested in surface Stokes drift velocities for our comparisons with the drifter-derived estimates. Given that OpenMetBuoys provide one-dimensional frequency wave spectra, thus lacking directional information, we simplify Equation 3 to (Breivik et al., 2014)

$$v_{\mathrm{st,dr}}(0) = \frac{2}{g}\int_0^{\infty} \omega^3 F(\omega)\, d\omega. \tag{4}$$

### 2.2. Wave Models and Satellite Observations

Table 1 outlines the configuration characteristics of the wave and current products used in our study. The operational Copernicus Mercator global ocean analysis and forecast system (Ferry et al., 2007) and the Copernicus ESA Globcurrent product (Rio et al., 2014) are considered for the surface current analysis. Mercator provides 6-hourly surface current data, whereas Globcurrent provides hourly estimates derived from a combination of Copernicus Marine Service near real-time satellite geostrophic surface currents and modeled Ekman drifts, utilizing European Center for Medium-Range Weather Forecasts (ECMWF) near real-time wind speed data. Both products ignore the effects of Stokes drift. To maintain consistency with the surface speeds recorded by the drifters, we consider only surface currents by setting depth to zero. Mercator's gridded data are available at a resolution of 1/12°, whereas Globcurrent has a resolution that is three times coarser 1/4°.

The surface Stokes drift and significant wave height are obtained from the MFWAM model (Aouf et al., 2019; Ardhuin et al., 2010; Janssen et al., 2014), an operational global ocean analysis and forecast system, and the ERA5 product (Hersbach et al., 2020). ERA5 combines historical observational data with advanced modeling techniques to produce reanalysis. This involves the assimilation of data from satellites, weather balloons, buoys, and ground stations. Specifically, ERA5 assimilates observations from SARAL and CryoSat-2 based on its operational stream (Hersbach et al., 2020). In contrast, MFWAM incorporates significant wave height observations from altimeters such as Jason-3, SARAL, CryoSat-2, Sentinel-3 A/B, CFOSAT, and Sentinel-6A as well as ocean-wave spectra from Sentinel-1 (Dalphinet et al., 2023). In terms of resolution, MFWAM provides 3-hourly instantaneous estimates with a spatial resolution of 1/12°. In contrast, ERA5 provides hourly data, thus enhancing temporal resolution by a factor of 3 compared to MFWAM. However, ERA5's spatial resolution is 6 times coarser at about 1/2°.

Notably, ERA5 does not incorporate surface current forcing, whereas MFWAM uses the operational Mercator forecast product. In particular, the standard MFWAM product is forced by surface currents from the global Mercator PSY4 ocean forecasting system, which provides daily updates. Given the differences in setup and

forcing systems between ERA5 and MFWAM, direct comparisons for evaluating current impact on wave evolution could be misleading. To address this, we conduct two additional experiments: one with MFWAM forced by the Globcurrent product and another without surface current data. This setup allows us to investigate the impact of currents on wave height by comparing three different MFWAM runs: one with model-derived currents (Mercator), one with satellite-derived currents (Globcurrent), and one excluding current data as shown in Table 1. Lastly, both the wave models and Globcurrent product are interpolated using the nearest neighbor technique to the drifters' locations accounting for the different sampling intervals of the GPS (30 min) and wave (3 hr) measurements.

## 3. A Comparative Analysis Along Drifters' Trajectories: Satellite Observations and Wave Models Against In Situ Measurements

### 3.1. Surface Current Velocity

Figure 2 presents maps of in situ-derived surface current speed along the drifter trajectories and those obtained by the Mercator and Globcurrent products. Compared to the drifters' measurements, both Mercator and Globcurrent appear to underestimate the surface current velocities within the core of the Agulhas Current and in areas beyond its retroflection, an observation previously reported for Globcurrent by Hart-Davis et al. (2018). The accompanying density plots, which include around 18,400 data points, show that this trend persists in both products when current speeds exceed approximately 0.5 m $s^{-1}$.

Globcurrent aligns more closely with drifter data, exhibiting a linear correlation of 0.84 and an RMSE (Root Mean Square Error) of 0.32 m $s^{-1}$. In contrast, Mercator displays a correlation of 0.51 and an RMSE of 0.52 m $s^{-1}$. The decomposition of the RMSE into bias and standard deviation (Murphy, 1988) reveals that bias has a negligible impact on the total error of the examined products (see Table A1, Appendix A).

These discrepancies can be partially attributed to the spatial and temporal resolution limitations of the products, which may not capture small-scale dynamics effectively. The observed underestimation of surface currents by the Mercator model aligns with findings in Mercator's Quality Information Document (Lellouche et al., 2023). This document indicates that when compared to in situ measurements from drifting buoys, the underestimation can range from 20% in strong currents to 60% in weak currents. Although the inclusion of Stokes drift, particularly during storms, may improve modeled surface velocities, its magnitude is expected to be relatively small in regions with strong currents, such as the Agulhas. This is because the current speeds in such areas are typically much higher than the Stokes drift, diminishing the latter's impact on the overall surface velocity. Globcurrent's performance, which partially depends on satellites' coverage and revisit period, may be constrained by its tendency to smooth small-scale dynamics affected by local wind variations and current variability (Hart-Davis et al., 2018).

Considering the variability in current strength in the study area, we analyze specific aspects for each drifter. Figure 3 presents scatter plots of surface speed for individual drifters, contrasting their measurements with those from the Mercator and Globcurrent products in the top and bottom panels, respectively. Notably, the four drifters deployed within the current core (AC-01, AC-02, AC-05, and AC-06) show significantly better alignment with Globcurrent, exhibiting linear correlation coefficients ranging from 0.79 to 0.86 compared to Mercator's 0.32 to 0.60. In contrast, drifters located around eddies exhibit varying correlation patterns. Mercator shows very weak correlations with coefficients of 0.10 and −0.11 for drifters ED-03 and ED-04, respectively, which are statistically well below the significance level. In contrast, Globcurrent maintains relatively good agreement, achieving moderate correlations of 0.58 and 0.77, respectively. As mentioned earlier, instances of near-surface inertial oscillations are revealed in Figure 1. These oscillations, driven by the Coriolis effect, lead to circular counterclockwise trajectories in the southern hemisphere and are particularly evident in the latter part of drifter ED-04's path.

### 3.2. Stokes Drift and Significant Wave Height

Although surface Stokes drift is expected to be significantly smaller than the geostrophic current in the Agulhas region, our primary focus is on evaluating the ERA5 and MFWAM operational products against in situ measurements. As shown in Figure 4, this analysis includes Stokes drifts derived from drifters, compared with ERA5 and MFWAM, along with their corresponding scatter plots. The analysis encompasses approximately 3,000 data points, which are notably fewer than those used in the surface current analysis. This is due to the less frequent sampling rate of wave spectra, which was set to 3 hr.

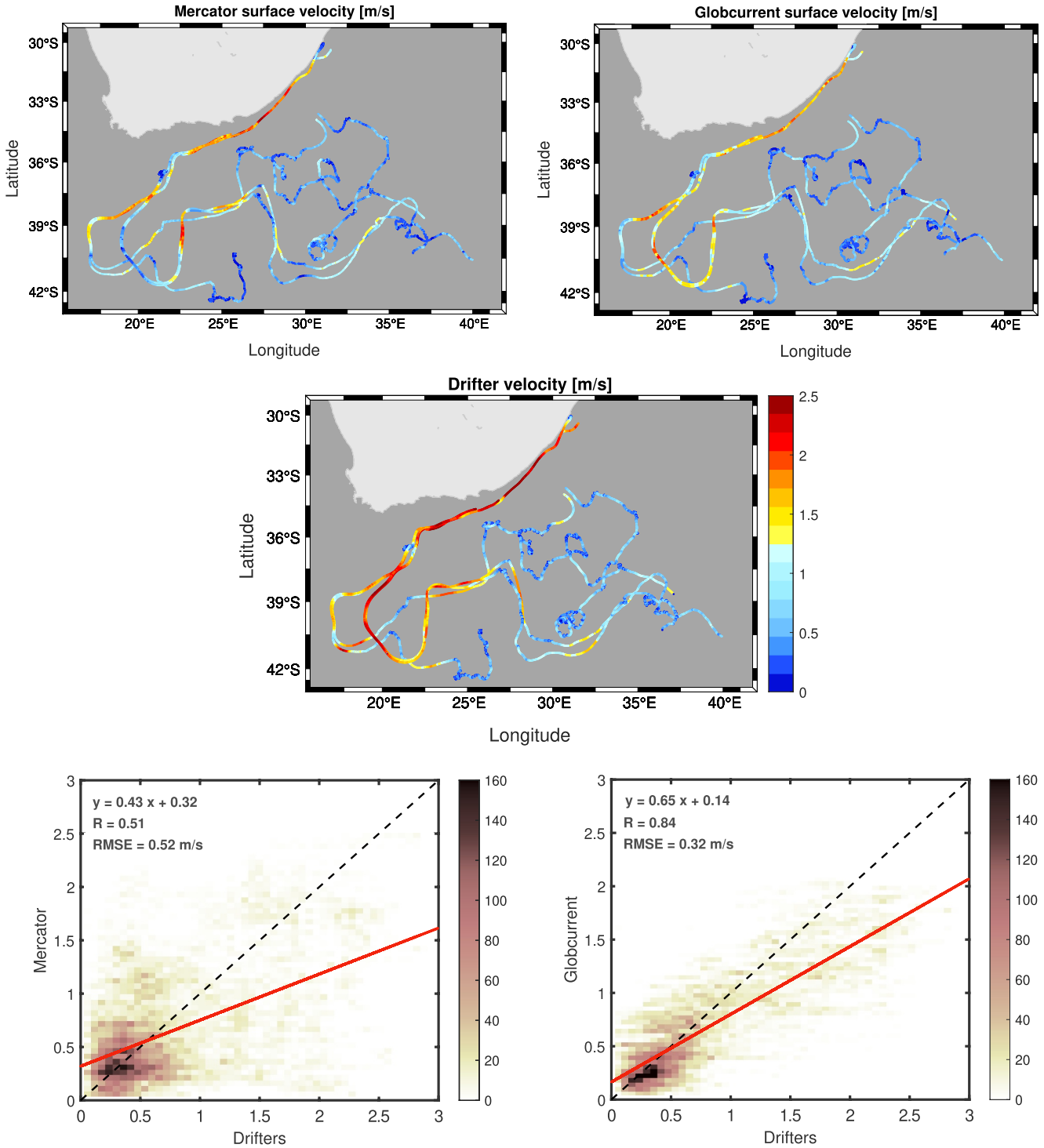


**Figure 2.** Surface current velocity interpolated along the six drifter trajectories from Mercator (top-left), Globcurrent (top-right), and as measured by the drifters (middle). Density plots of drifters' measurements versus Mercator (bottom-left) and Globcurrent (bottom-right). A regression line is shown in red color. The dashed black line represents the line of equality when in situ = model. Unit: $[ms^{-1}]$.

The drifters recorded surface Stokes drifts reaching up to approximately 0.3 m $s^{-1}$ with both models consistently overestimating these values. Particularly ERA5 shows a pronounced tendency toward higher estimates. In evaluating model performance via correlation coefficients, both models demonstrated a reasonable alignment with drifter data: MFWAM achieved a correlation of 0.80, while ERA5 recorded a lower correlation of 0.72 albeit

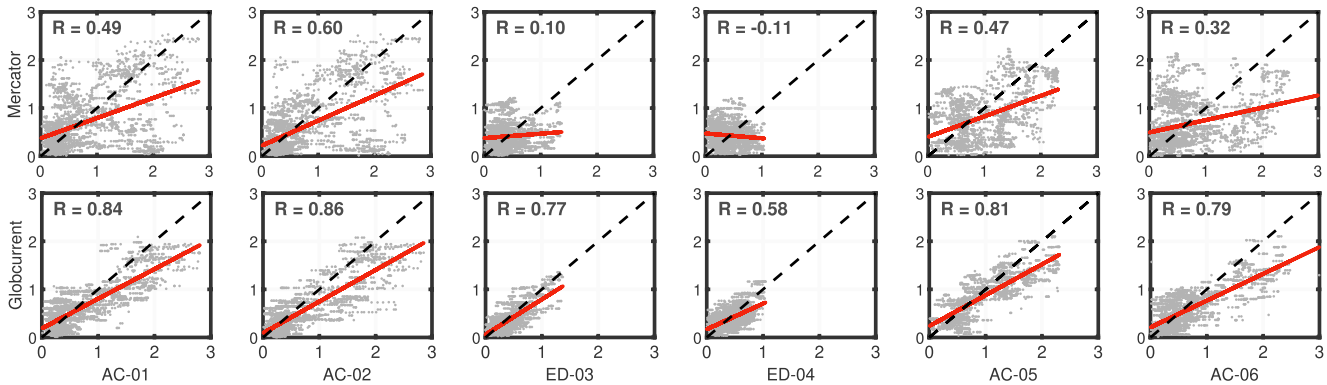


**Figure 3.** Scatter plots of drifter-derived surface current velocity versus Mercator (top panels) and Globcurrent (bottom panels) for each drifter separately. A regression line is shown in red color. The dashed black line represents the line of equality when in situ = model. Unit: m $s^{-1}$.

accompanied by notable variability. In terms of accuracy, assessed through RMSE, both models perform similarly, achieving 0.04 and 0.05 m $s^{-1}$ for MFWAM and ERA5, with bias and standard deviation being comparable (see Table A1, Appendix A).

Note that as reported by Breivik et al. (2014) and Ardhuin et al. (2009), implementing an unidirectional approach may result in an overestimation of the Stokes drifts by approximately 15%–19%, whereas in swell-dominated seas the impact is less. Therefore, this would lead to relatively larger discrepancies compared to wave models. However, given that the observed Stokes drifts do not exceed 0.3 m $s^{-1}$, and considering that geostrophic forces, being predominant, can nearly be 10 times stronger, the influence of our assumption is likely minimal. Thus, we deem this assumption to fall within the noise level of our measurements (Rabault et al., 2023), rendering its impact negligible.

Various factors could contribute to the observed discrepancies, including differences in wave model setup and forcing parameters. For example, the relatively coarse spatial resolution of 1/2° in ERA5 might fail to capture small-scale dynamics influenced by local wind variations aligning with the observed average Stokes drift direction (Clarke & Van Gorder, 2018). An individual analysis of the drifters' trajectories indicates a comparable level of overestimation across all data points, with linear correlations ranging from 0.69 to 0.85 for both models, with MFWAM achieving approximately 10% higher correlation. Detailed plots of these correlations can be found in Appendix A (see Figure A1).

Similar to the analysis of Stokes drifts, Figure 5 presents maps of significant wave height estimates as derived from both models against drifters. The maps suggest good correspondence for both models. In particular, correlations of 0.90 and 0.83 and RMSE of the differences at 0.39 and 0.54 m are calculated between the drifters and MFWAM and the drifters and ERA5, respectively. Notably, ERA5 exhibits larger discrepancies and a distinct trend of underestimation with increasing wave height, particularly for waves exceeding approximately 2.5 m. This trend can by described by a negative bias of 0.23 m for ERA5, compared to 0.04 m for MFWAM, whereas in terms of variability the standard deviation is estimated at 0.48 and 0.38 m, respectively (see Table A1, Appendix A).

A considerable part of the underestimation in both MFWAM and ERA5 appears to be linked to the surface current strength as indicated by the coloring of the scatter points based on drifter-measured current speeds. In particular, ERA5 does not incorporate surface current data into its simulations, overlooking the impact of currents on wave evolution. Specifically, ERA5's lack of accounting for wave refraction and steepening effects leads to larger discrepancies compared to MFWAM with errors occasionally exceeding 2 m in extreme sea states. This observation underscores the critical role of incorporating current modeling within wave forecasting systems. An individual significant wave height analysis of the drifter trajectories reveals similar trends to Figure 5 with linear correlations ranging from 0.73 to 0.95 (see Figure A2, Appendix A). MFWAM consistently outperforms ERA5, confirming the impact of current and eddies on wave height forecasts.

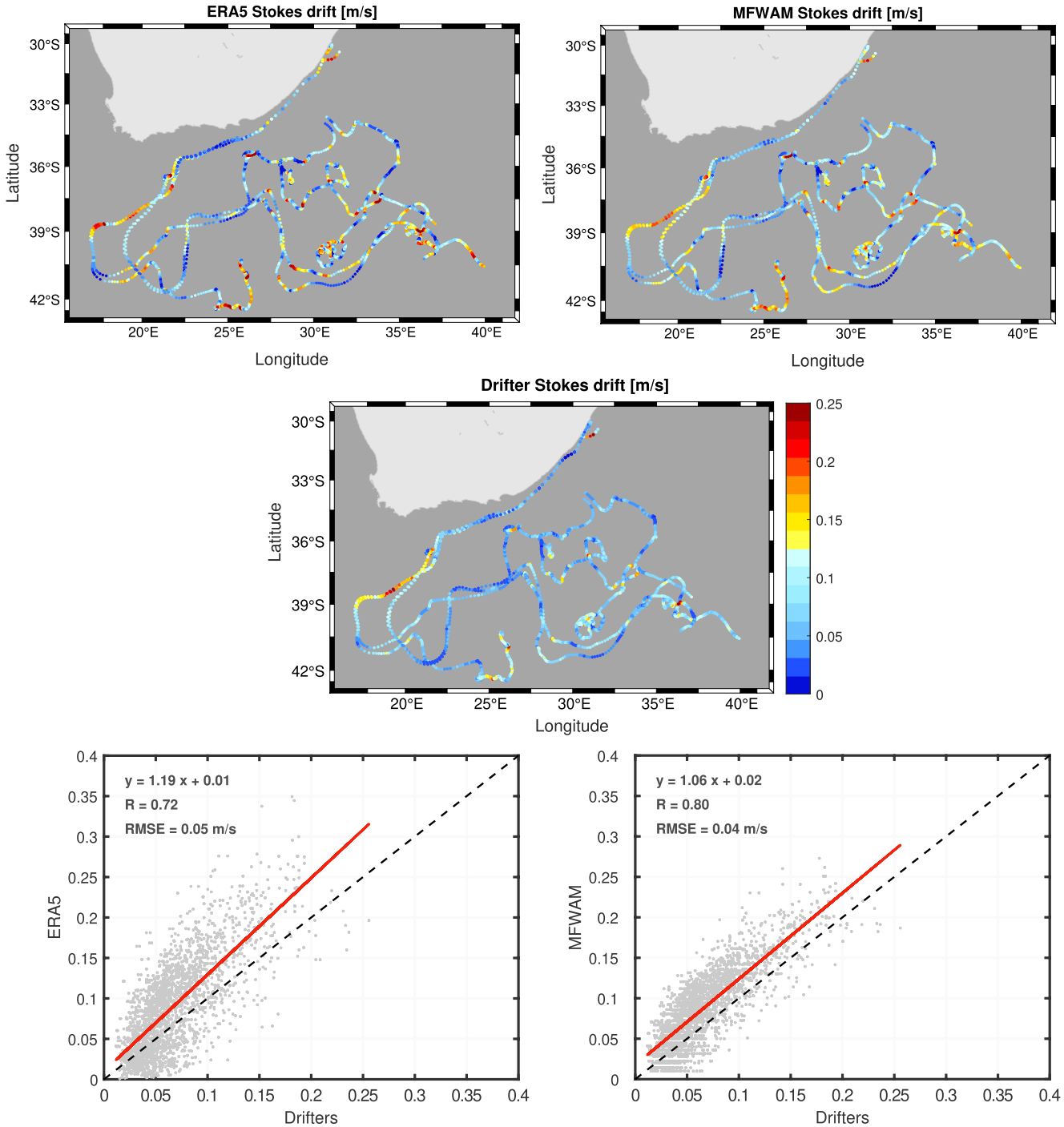


**Figure 4.** Surface Stokes drifts interpolated along the six drifter trajectories from ERA5 (top-left), MFWAM (top-right), and as measured by the drifters (middle). Scatter plots of drifters' measurements versus ERA5 (bottom-left) and MFWAM (bottom-right). A regression line is shown in red color. The dashed black line represents the line of equality when in situ = model. Unit: m $s^{-1}$.

A comparison between significant wave height and Stokes drift results reveals contrasting trends: although significant wave heights are underestimated, Stokes drift shows a tendency to be overestimated with increasing sea states. In our study area, wave heights are primarily dominated by swells generated from distant storms. The underestimation of wave heights in high sea states suggests that wind speeds during these storm events may be underestimated, creating uncertainties in the initial wind-waves growth conditions and, consequently, affecting

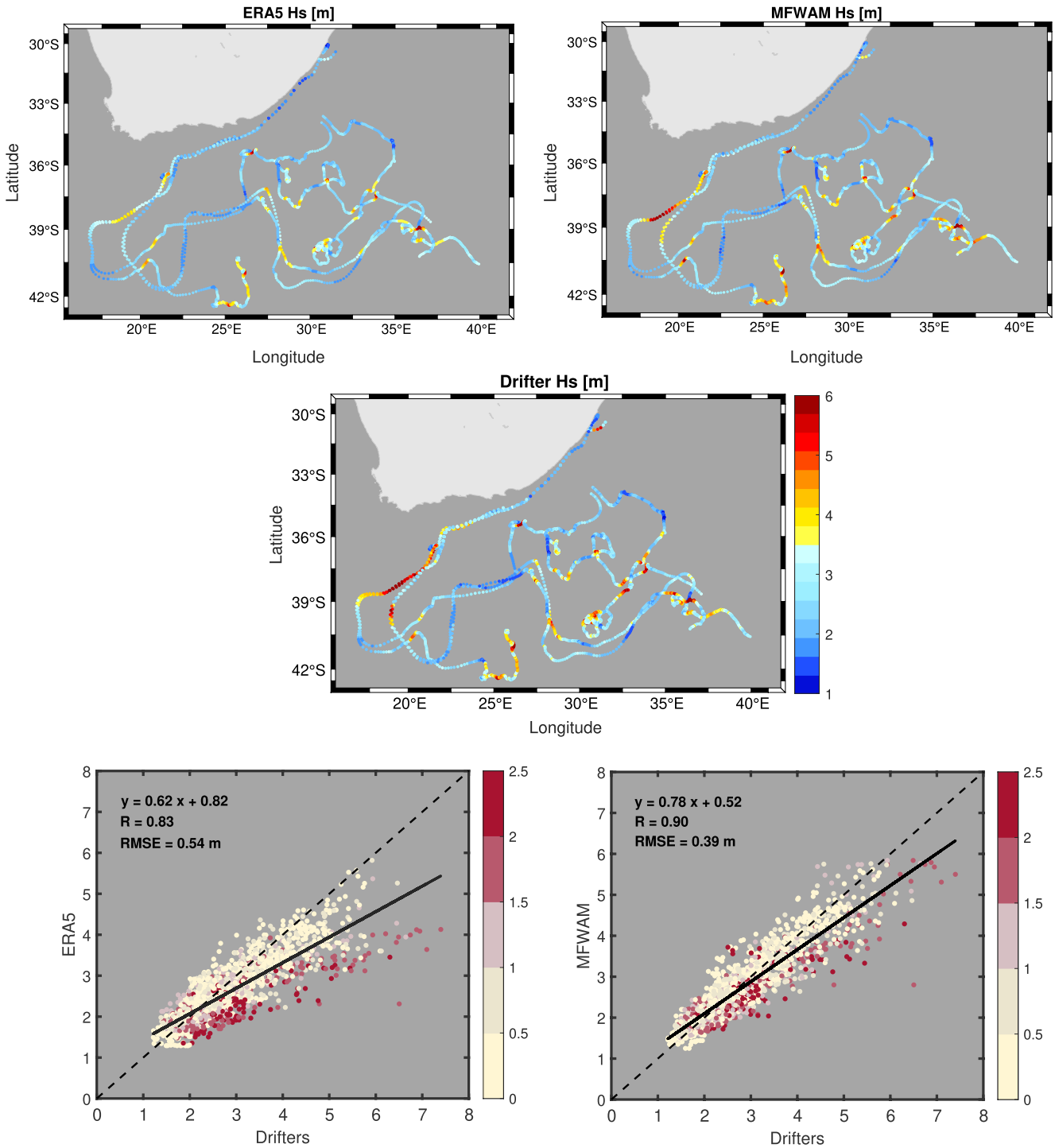


**Figure 5.** Significant wave height interpolated along the six drifter trajectories from ERA5 (top-left), MFWAM (top-right), and as measured by the drifters (middle). Scatter plots of drifters' significant wave height measurements versus ERA5 (bottom-left) and MFWAM (bottom-right) colored to indicate the drifters' surface current speeds $v_{dr}$ $\left(\mathrm{m\ s^{-1}}\right)$. A regression line is shown in black color. The dashed black line represents the line of equality when in situ = model. Unit: m.

the transition to swell regime. In contrast, the overestimation of Stokes drift can be attributed to the use of a Phillips wave spectrum shape for the high-frequency part of the spectrum in both ERA5 and MFWAM, which tends to distribute excess energy in this range (Breivik et al., 2016). Additionally, the upper frequency cutoff for both models is significantly higher than that of the drifters (0.56 Hz for MFWAM and 0.55 Hz for ERA5, compared to 0.30 Hz for the drifters). Taking into account that Stokes drift estimates are sensitive to high-

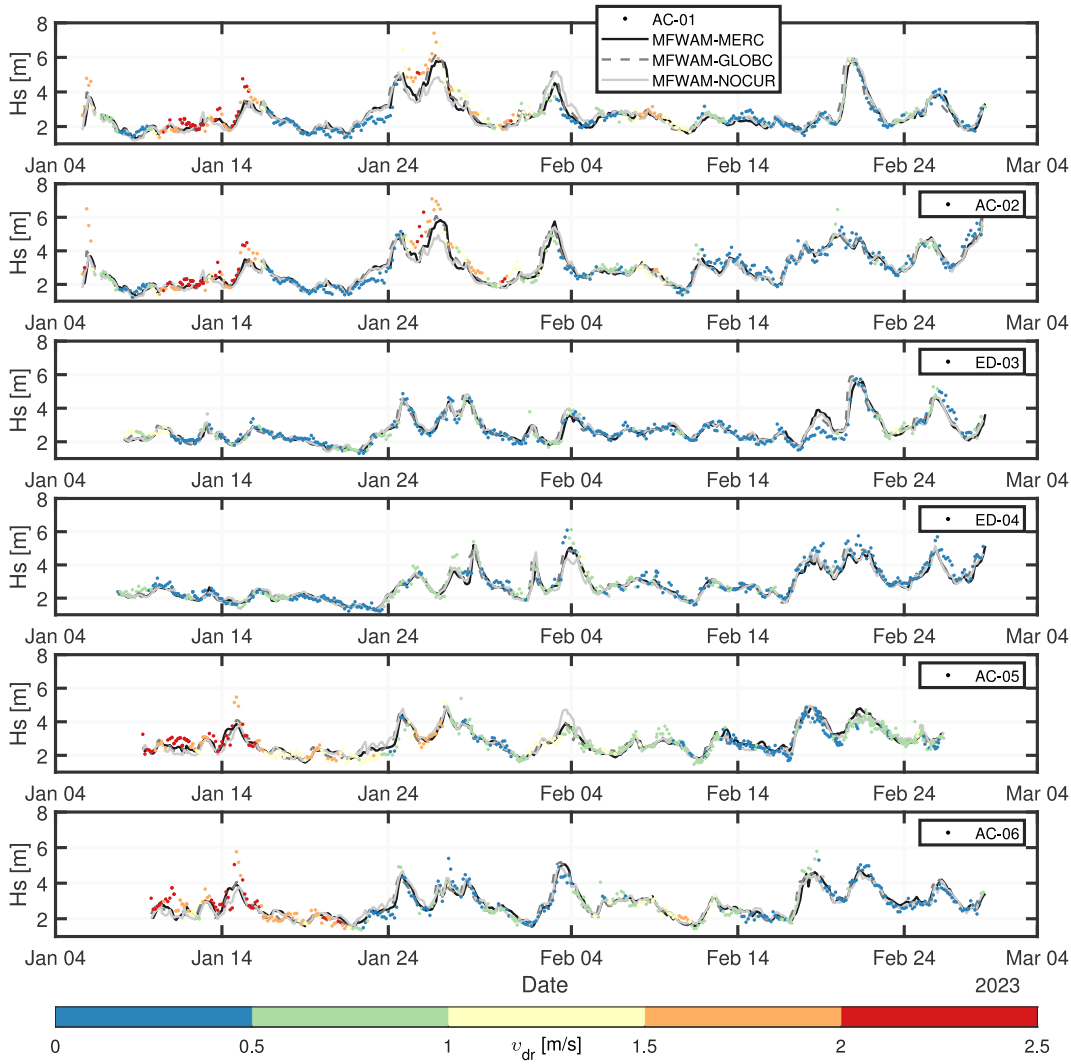


**Figure 6.** Time series of significant wave height derived from each drifter and the MFWAM products. The wave heights measured by the drifters are shown as dots colored to indicate the corresponding surface current speeds ($v_{dr}$).

frequency components—magnified by the $\omega^3 = (2\pi f)^3$ factor (Equation 4)—this suggests that noise will propagate into the final estimates, thereby amplifying inaccuracies.

Given the inherent complexities of absolute comparisons between different models, which are developed using varied wind, wave, and current forcing systems along with different spatial and temporal resolutions as shown in Table 1, such comparisons can admittedly complicate interpretation of differences. Although geostrophic currents dominate in the region, we must also acknowledge topographic steering and wind-driven small-scale ageostrophic components that are captured by the drifters but not necessarily by the models. Lastly, errors related to instrument performance and method implementation may also contribute to RMSE. Therefore, the next section discusses additional experiments, customizing MFWAM with different current forcing settings to assess the potential weaknesses and strengths inherent in each scenario.

## 4. Surface Current Impact on Wave Parameters and Ocean Wave Spectra

### 4.1. Significant Wave Height and Stokes Drift

In this experiment, MFWAM is run with (a) the Mercator surface current product, (b) the Globcurrent surface current product, and (c) without currents. Figure 6 illustrates the fluctuations in significant wave heights along the path of each drifter per model from the date of deployment until February 28.

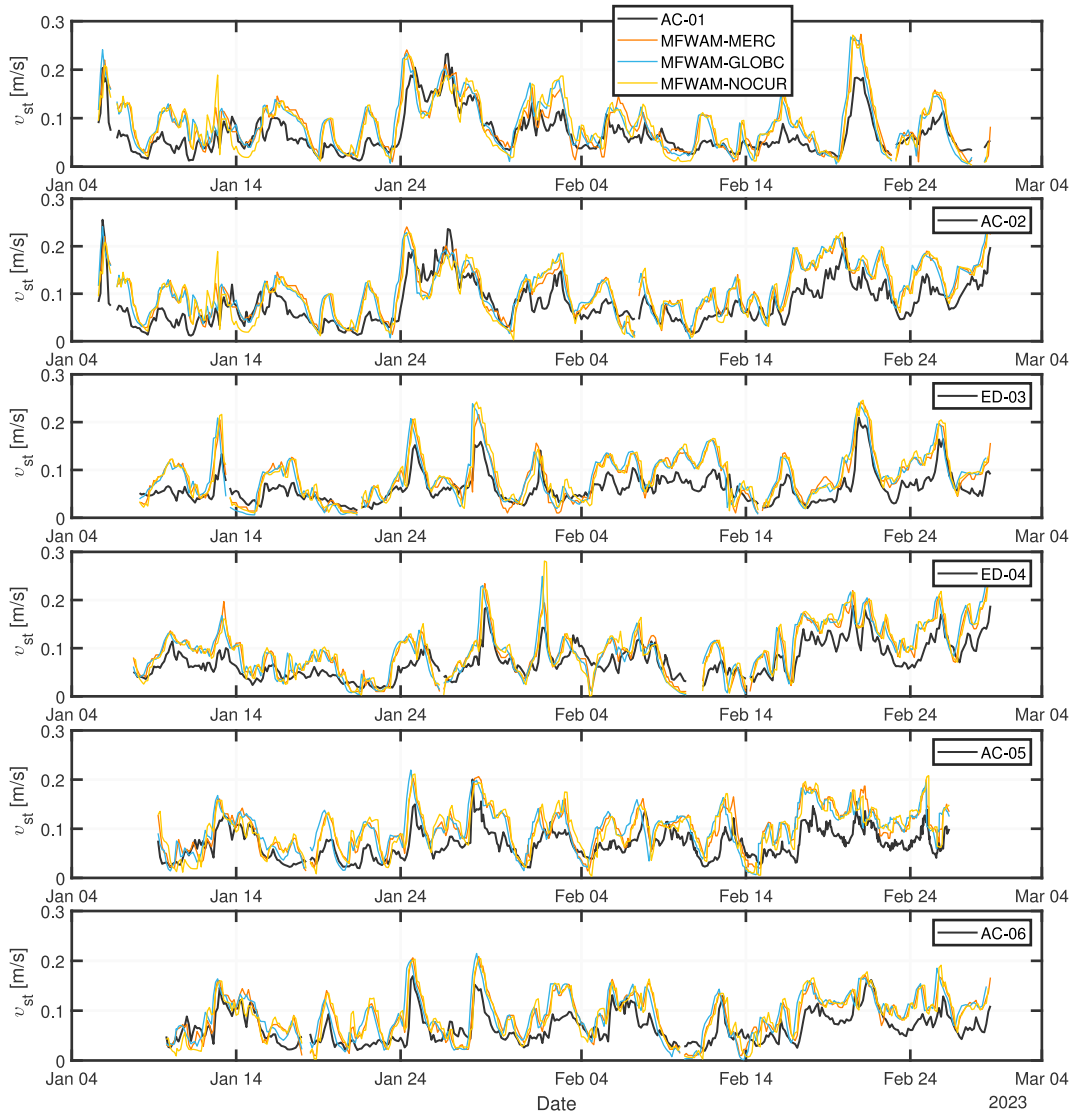


**Figure 7.** Time series of Stokes drift ($v_{st}$) derived from each drifter and customized MFWAM runs indicated by the different colors.

Overall, in relatively calm current conditions ($<0.5$ m s$^{-1}$) and up to moderate significant wave height ($<3$ m), the model runs align closely with in situ measurements. However, under higher wave conditions—particularly when wave heights exceed 4 m, likely indicating storm events—the models begin to diverge with increasing current speed. For instance, drifter AC-01 recorded two significant wave height peaks of around 6 m at the end of January and February, while experiencing current speeds above 1.5 m s$^{-1}$ and below 1.0 m s$^{-1}$, respectively. Notably, the first peak was also recorded by drifter AC-02. These instances indicate a pronounced underestimation of wave height associated with increased drifter speeds. This suggests that higher current speeds likely introduce significant uncertainties in wave forecasts when currents are not considered with discrepancies sometimes exceeding 2 m in high sea states as also shown in the analysis of ERA5 data (Figure 5) and further illustrated in Figure A3 of Appendix A. Conversely, the MFWAM run excluding current data can lead to an overestimation of wave height as observed for AC-05 on February 3. This can be attributed to the alignment between wave and currents in this case with a mean wave direction of 232° relative to North according to MFWAM and a current flow direction of 223° based on Globcurrent. When waves and currents propagate in the same direction the momentum flux to the waves is reduced, and, consequently, the exclusion of current in modeling can result in an overestimation of wave heights (Ponce de León & Guedes Soares, 2021). The impact of

not including current data in the simulations is also evident in the RMSE, which increases to 0.45 m compared to 0.39 m when Mercator and Globcurrent current data are integrated into the model (see Table A1, Appendix A). This result also suggests that both Mercator and Globcurrent perform equally well compared to drifters when current dynamics are considered.

Continuing our analysis of Stokes drifts, Figure 7 compares in situ measurements with the customized MFWAM results. Although all model runs generally capture the overall in situ trends, a systematic overestimation is evident across the models. A comparison between MFWAM-Mercator, MFWAM-Globcurrent, and MFWAM-no-current runs reveals that current forcing has only a marginal impact, as Stokes drift is primarily driven by local winds. This suggests that the inclusion of current data does not significantly impact the overall accuracy of Stokes drift predictions. Overall, the discrepancies observed across the model experiments seem to be within the noise level with the RMSE calculated to be about 10% of the mean modeled Stokes drifts, suggesting a relatively minor but still noticeable variance (see Table A1, Appendix A).

As previously mentioned, Globcurrent is produced by combining geostrophic velocities, derived from altimeters, with modeled Ekman drifts, while neglecting the impact of Stokes drift. Given that Stokes drift reaches up to approximately 0.3 m $s^{-1}$ according to our analysis, its contribution to the overall surface velocity is expected to be small. However, in scenarios with weaker currents, incorporating Stokes drift could potentially improve the agreement between satellite observations and in situ measurements.

### 4.2. Ocean Wave Spectra

Taking into account the influence of currents on the wave field and the resulting energy transfer, we will now investigate the wave spectra computed by all three model experiments and drifters to highlight their impact. We focus on three areas for detailed examination, and for simplicity, we concentrate on data from a single drifter, namely AC-01. As shown in Figure 1, this drifter followed the Agulhas current core experiencing a wide range of current speeds, allowing us to evaluate the impact of varying current conditions. Averaged Mercator and Globcurrent surface velocities over the experiment period are shown in the top-left and top-right maps of Figure 8, respectively. The examined zones are around the core of the Agulhas Current (zone A) and its retroflection (zones B and C). All cases represent collocations within 1 hr and 20 km distance between gridded MFWAM points and drifter locations to minimize the impact of local wind-wave condition differences. The unidirectional wave spectra from both drifters and MFWAM runs (panels a–c) as well as the MFWAM directional (panels d–l) wave spectra reveal distinct patterns and variations.

In zone A, with current speeds reaching about 2.4 m $s^{-1}$, swells travel northeast at 41.7°, whereas long-period wind waves come from the opposite direction at 192.8°. The one-dimensional wave spectra provided by model runs with Globcurrent and Mercator closely match the drifter's significant wave height estimates with discrepancies of 2 and 32 cm, respectively (panel a). Ignoring current refraction results in a more peaky wave spectrum for both swell and wind waves and an overestimation of the significant wave height by 73 cm. The impact of currents on waves is also captured in the MFWAM directional spread where wave energy is spread across frequencies and directions due to refraction (panels d, g vs. j). Notably, wave energy decreases when current refraction is included, an observation that has also been reported in other studies (Ponce de León & Guedes Soares, 2021; Rapizo et al., 2018). It is evident that when currents are accounted for, swells with a peak wave period of about 13 s are slightly shortened to 12 s under a current strength of 2.4 m $s^{-1}$ without noticeable impact on their propagation direction.

In zone B, within the retroflection area, the current strength decreases to 1.6 m $s^{-1}$. Swells dominate, traveling northeast at 51.6°, whereas wind waves are much weaker, traveling east-west at 89.9°. The drifter records a significant wave height for the swell at 7.4 m with its one-dimensional wave spectrum featuring a high-energy swell peak nearly 4°times larger than those reported by all model runs, indicating a considerable underestimation of the significant wave height (panel b). Specifically, Mercator and Globcurrent underestimate the wave height by 1.9 and 1.4 m, respectively. Without current data, the underestimation reaches 2.6 m, a critical magnitude for accurate wave forecasting and marine safety. Overall, the observed wave height variability underscores the challenges of modeling dynamic marine environments and the need for ongoing refinement of model parameters especially in extreme wave conditions. In contrast to zone A, the directional wave spectra show

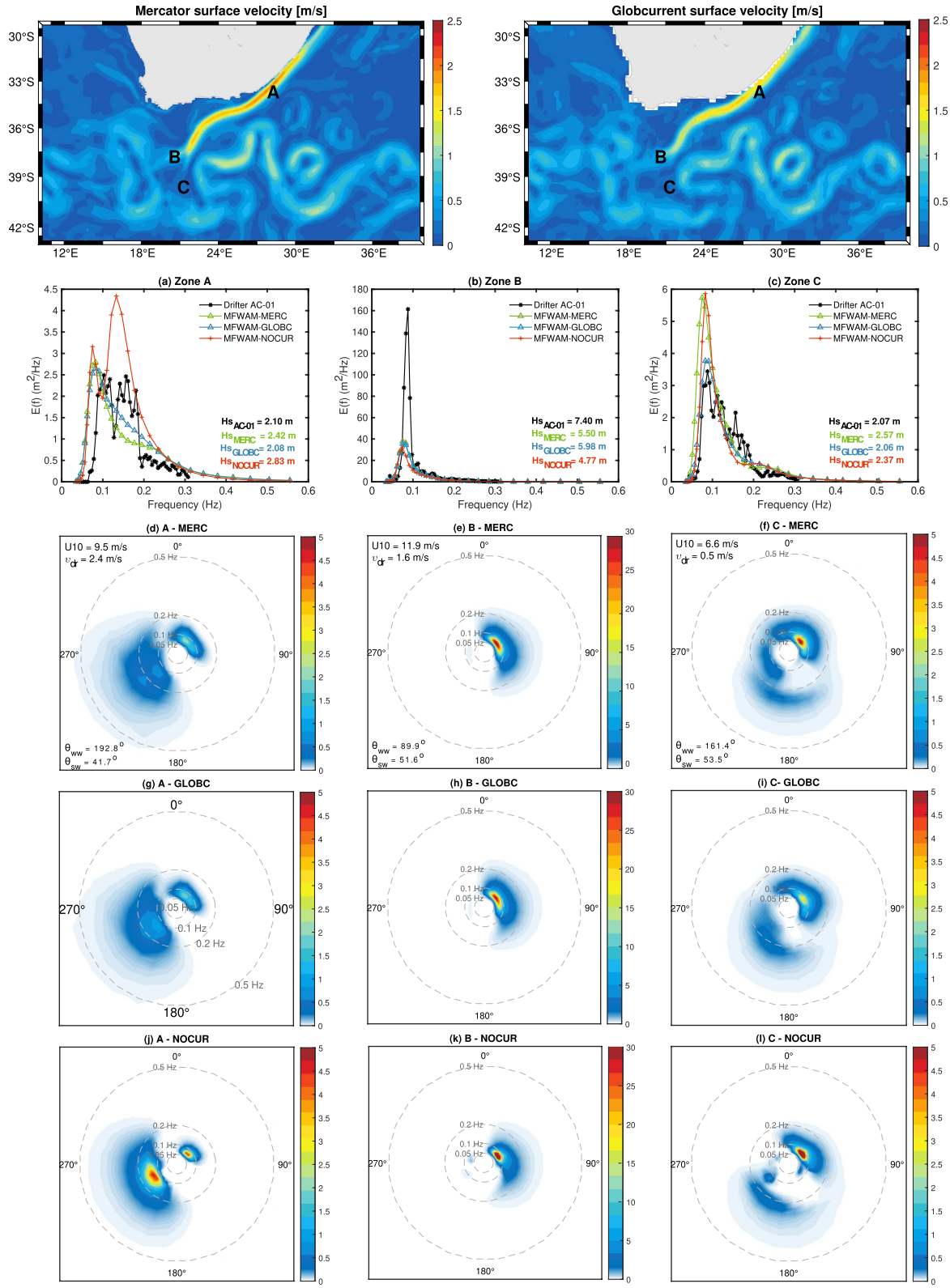


**Figure 8.** Maps of the Mercator (top-left) and Globcurrent (top-right) surface velocities averaged over January–February 2023. MFWAM and drifter-derived unidirectional (a–c) and MFWAM directional (d–l) wave spectra in the current core (A) and its retroflection (B, C) using Mercator (MERC), Globcurrent (GLOBC) and without current forcing (NOCUR). Parameters: MFWAM wind wave direction ($\theta_{ww}$) and primary swell direction ($\theta_{sw}$), ERA5 wind speed ($U10$) and drifter derived surface speeds ($\upsilon_{dr}$).

minor signs of wave energy spread, indicating that swells of the same order of magnitude, that is, 13 s, can maintain their wavelength and propagation direction when current speeds reach 1.6 m $s^{-1}$ (panels e, h vs. k).

Continuing with the retroflection area, zone C involves a much weaker current approximately 0.5 m $s^{-1}$. Similar to zone A, swells travel northeast (53.5°), while a weaker wind sea originates from the opposite direction (161.4°). The significant wave height is recorded at 2.07 m with Globcurrent providing an accurate forecast at 2.06 m (panel c). In contrast, both the Mercator and no-current scenarios reveal larger wave energy peaks, leading to wave height overestimations by 50 and 30 cm, respectively. Signs of wave energy spread are still evident when currents are included in the directional wave spectra, but they are much less pronounced than in zone A due to the weaker current strength (panels f, i vs. l). In terms of swell modulations, the MFWAM-Globcurrent run aligns well with the no-current scenario, showing a 12-s peak wave period compared to 13 s for the MFWAM-Mercator product. However, the MFWAM-Globcurrent wave spectrum reveals a significant decrease in wave energy around the peak period. Consulting the drifter one-dimensional wave spectrum, it is evident that the MFWAM-Globcurrent run demonstrate better alignment with the drifter measurements.

Overall, the analysis of wave spectra between the standard MFWAM runs, using the Mercator current product and those computed after forcing the wave system with satellite observations, that is, Globcurrent, reveals that the latter shows better agreement with the in situ measurements. As discussed in detail in Section 3.1, the Mercator product underperforms compared to Globcurrent, showing extreme variability in the region of interest. Specifically, for drifter AC-01, which this analysis examines, the correlation between the drifter and the model was calculated at 0.49, while Globcurrent achieved a significantly higher correlation at 0.84 (Figure 3). Furthermore, some observed discrepancies can be attributed to Mercator's inability to effectively resolve mesoscale vorticity (Ponce de León & Guedes Soares, 2021). This shortfall may lead to significant errors particularly in regions with strong currents such as the Agulhas region.

## 5. Current-Induced Wave Modulation Signatures in Satellite Altimetry

As previously mentioned, wave refraction is not a local process. Waves continue to be modulated by currents many kilometers away from their initial point of interaction (Halsne et al., 2023). Although drifters are useful for validation and calibration activities and essential for localized wave field monitoring, using them to monitor and study the impact of refraction across wide areas is impractical as one would need to deploy hundreds of drifters simultaneously to effectively capture its spatial extent. To investigate wave refraction on a broader scale, we use the Global Ocean L3 1-Hz significant wave height product from near-real-time satellite observations. This data set includes data from Sentinel-3A/B, Sentinel-6, CFOSAT, ALTIKA, CryoSat-2, HY-2B, and Jason-3. These satellites provide comprehensive coverage that enables a detailed analysis of wave refraction patterns over extensive geographic areas and under various conditions.

To evaluate the performance of the satellites against drifters, we first conducted a comparative analysis. For the mono-mission satellite-based along-track significant wave height measurements, collocations were implemented using constraints of a 15-min time window and a 20-km radius around each independent drifter record using the open-source WAVY software (https://github.com/bohlinger/wavy, Bohlinger et al. (2019)). Figure 9 illustrates the significant wave height time series, demonstrating a good agreement between in situ measurements and satellite observations across a wide range of wave conditions and regardless of whether the sensors were positioned around the core of the current or its associated eddies.

To quantify this agreement, a comparison of the closest satellite records to each drifter position was performed, revealing a correlation of 0.97 and an RMSE of 24 cm. Since no interpolation was applied to match the exact drifter positions, part of the discrepancies may be attributed to wave height modulations induced by wave-current interactions, including refraction effects that continue to develop several kilometers away from the drifters' locations. It is noteworthy that the satellites demonstrate good performance even in high sea-state conditions. For instance, Sentinel-3A and Jason-3 along with Altika measured wave heights up to 6 m on January 24 and February 20, respectively, observations in line with drifter AC-01's measurements. Similarly, between 25 and 29 January CFOSAT, CryoSat-2, Jason-3, and Altika captured wave heights of approximately 4.5 and 5 m around the eddies, aligning well with the measurements from drifters ED-03 and ED-04.

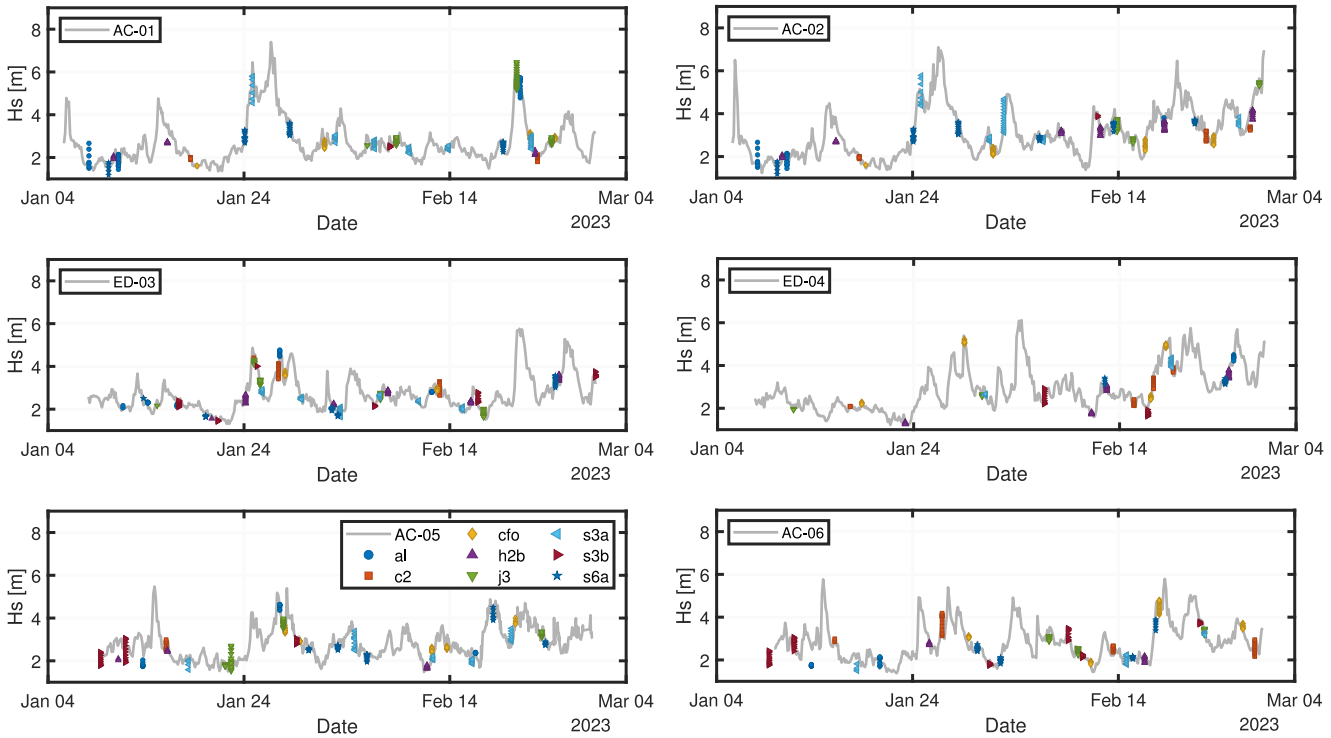


**Figure 9.** Time series of significant wave height measurements per drifter along with collocated satellite altimetry observations obtained from the Copernicus Global Ocean L3 Significant Wave Height product (1 Hz). Collocation criteria: 20 km and 15 min around each drifter measurement point. The satellite observations from Altika-SARAL (al), CryoSat-2 (c2), Jason-3 (j3), CFOSAT (cfo), HY-2B (h2b), Sentinel-3A/B (s3a/s3b), and Sentinel-6A (s6a) are color coded.

Figure 10 provides insights into the evolution of refraction. Estimates of significant wave heights along the paths of drifters AC-05 (left panel) and ED-03 (right panel) are illustrated, superimposed on Mercator current velocities averaged over the period January–February 2023. In this deepwater region, collocated altimeter tracks extend hundreds of kilometers from the drifters' points, demonstrating how the wave heights are

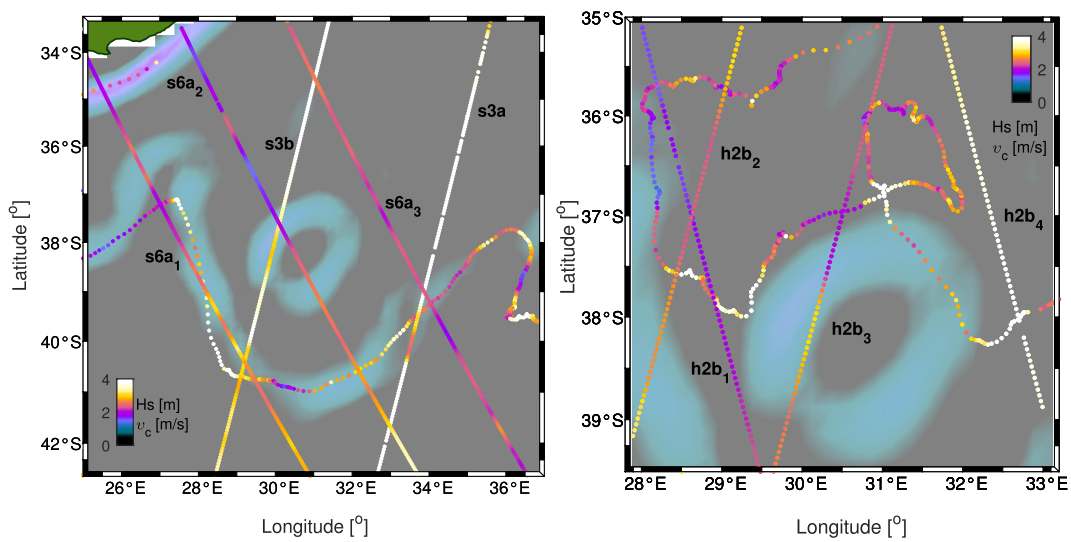


**Figure 10.** Mean Mercator current velocities with superimposed significant wave height estimates from drifter AC-05 (left panel) between 9 January 2023 and 28 February 2023 and from drifter ED-03 (right panel) between 9 January 2023 and 20 February 2023. Collocated altimetry data from Sentinel-3A/B (s3a/s3b), Sentinel-6A (s6a), and HY-2B (h2b) are also illustrated using as criterion a 15-min acquisition time difference between satellite observations and drifters' measurements.

modulated by the Agulhas Current and its surrounding eddies. Notably, waves, regardless of their initial height, exhibit pronounced modulations when traversing the area of current return and the observed eddy. In contrast, tracks that span regions outside the influence of the current, where surface speeds are reported below 0.5 m $s^{-1}$ (h2b1, h2b4), show only minor variations in wave height. Within the eddies, waves are observed to either steepen ($h2b_3$) or flatten (s3b). Several studies have reported that these dynamics are significantly influenced by the direction in which the waves encounter the current (Ardhuin et al., 2009; Ponce de León & Guedes Soares, 2021; Quilfen & Chapron, 2019). Considering the additional information acquired by the drifters in our study, this collocation experiment provides clear evidence of the importance of using multi-source data to map the complex interactions between waves and currents as well as their spatial extent in regions with strong currents.

## 6. Conclusions

This study has investigated in situ wave measurements collected in the Agulhas Current during the ESA-PECO2 Advanced Ocean Training Course 2023, part of the One Ocean Expedition 2021–2023, to evaluate the influence of wave-current interactions on wave models and altimetry-derived products. In January 2023, six OpenMetBuoy drifters were deployed in the Indian Ocean in and around the Agulhas Current. Over approximately 2 months, these drifters recorded wave spectra and their location, enabling the estimation of significant wave height and Stokes drift along their paths. Additionally, drifter speeds were estimated using GPS data, allowing estimates of surface current speeds, as the drifters experienced minimal direct windage due to their high immersion ratio.

The analysis first focused on surface current products. The Copernicus ESA Globcurrent product combines altimetry-derived geostrophic currents with Ekman drift computed from atmospheric forecasts. We found that this product tends to underestimate surface velocities exceeding approximately 0.5 m $s^{-1}$. A similar underestimation with a significantly greater variability was observed for the Mercator surface current product. Moreover, circular trajectories indicative of inertial oscillations were observed over periods of days likely driven by rapid changes in wind speed and direction.

Further, we compared modeled surface Stokes drift and significant wave height from ERA5 and MFWAM with the in situ measurements. ERA5 consistently underestimated significant wave heights over 2.5 m, whereas MFWAM demonstrated good agreement with drifter data. Both models tended to overestimate the Stokes drift with ERA5 showing greater variability. The absence of current forcing in ERA5, coupled with its coarser spatial resolution (1/2°) compared to MFWAM (1/12°), likely contributes to the decreased accuracy of ERA5 in areas with strong currents, emphasizing the complexities and challenges in accurately modeling wave-current interactions in dynamic regions such as the Agulhas Current.

A customized MFWAM run, which excludes current forcing, revealed an underestimation of wave height, occasionally exceeding 2 m as current velocities increase compared to drifter current estimates. A comparison of the directional MFWAM wave spectra, both with and without current data, demonstrated how current-induced refraction alters the shape of the wave spectra. The refraction bends the waves, causing them to become steeper or flatter and directionally more spread. Furthermore, the MFWAM model forced with Globcurrent surface currents tends to align closely with drifter observations and even outperforms the operational MFWAM model that uses Mercator-derived currents.

The study concludes with a comparative analysis of significant wave heights from the drifters with those from collocated satellite altimeter observations from various missions showing good correspondence. Notably, current-induced wave refraction patterns are observed along the satellite tracks with wave heights being significantly modulated when crossing eddies or the current core. These findings highlight the need for high-resolution models and multisource data integration to achieve accurate wave forecasts.

Lastly, the authors would like to emphasize that the data analyzed in this study were collected during the Australian summer, a period with comparably milder storm activity relative to the winter season in the southern region. A year-round field campaign would be necessary for a comprehensive validation of satellite products and models, as it would capture a wider spectrum of sea states and current variability, including extreme conditions associated with storm periods, where the examined products demonstrated increased sensitivity.

## Appendix A

This section provides supplementary information regarding the analyses between wave models, satellite observations, and in situ measurements. In particular, Figure A1 presents scatter plots illustrating the relationship between Stokes drift values estimated by drifters and those estimated by the ERA5 (top panels) and MFWAM (bottom panels) models. Each subplot represents collocated data in both time and space for each drifter separately. The scatter plots highlight the areas of agreement and discrepancy, providing a visual representation of models performance.

Similarly, Figure A2 depicts scatter plots for significant wave height, comparing the drifter measurements with those derived from the ERA5 (top panels) and MFWAM (bottom panels) models.

Table A1 summarizes statistics of all examined scenarios. Key metrics, including root mean square error (RMSE), mean (bias), and standard deviation (Std. Dev.), provide a quantitative assessment of the performance of all the examined current and wave products against drifters. The correlation coefficients (Corr. Coef.) further indicate the strength of the linear relationship between models, satellite observations, and in situ measurements. In addition, Figure A3 presents scatter plots of significant wave height (left-panel) and Stokes drifts (right-panel) as obtained from the drifters and the customized MFWAM runs.

**Table A1**
*Statistics of the Differences and Correlation Coefficients of Wave Models and Satellite-Derived Products Against In Situ Measurements From the OpenMetBuoy (OMB) Drifters*

| | Bias | Std.Dev. | RMSE | Corr. Coef. (−) |
|---|---|---|---|---|
| Surface current speed $[\mathrm{m\ s^{-1}}]$ | | | | |
| Mercator − OMB | −0.06 | 0.52 | 0.52 | 0.51 |
| Globcurrent − OMB | −0.09 | 0.31 | 0.32 | 0.84 |
| Surface Stokes drift $[\mathrm{m\ s^{-1}}]$ | | | | |
| ERA5 − OMB | 0.03 | 0.04 | 0.05 | 0.72 |
| $\mathrm{MFWAM_{MERC}}$ − OMB | 0.02 | 0.03 | 0.04 | 0.80 |
| $\mathrm{MFWAM_{GLOBC}}$ − OMB | 0.03 | 0.03 | 0.04 | 0.75 |
| $\mathrm{MFWAM_{NOCUR}}$ − OMB | 0.03 | 0.03 | 0.04 | 0.78 |
| Significant wave height [m] | | | | |
| ERA5 − OMB | −0.23 | 0.48 | 0.54 | 0.83 |
| $\mathrm{MFWAM_{MERC}}$ − OMB | −0.04 | 0.38 | 0.39 | 0.90 |
| $\mathrm{MFWAM_{GLOBC}}$ − OMB | −0.04 | 0.39 | 0.39 | 0.91 |
| $\mathrm{MFWAM_{NOCUR}}$ − OMB | −0.06 | 0.45 | 0.45 | 0.88 |

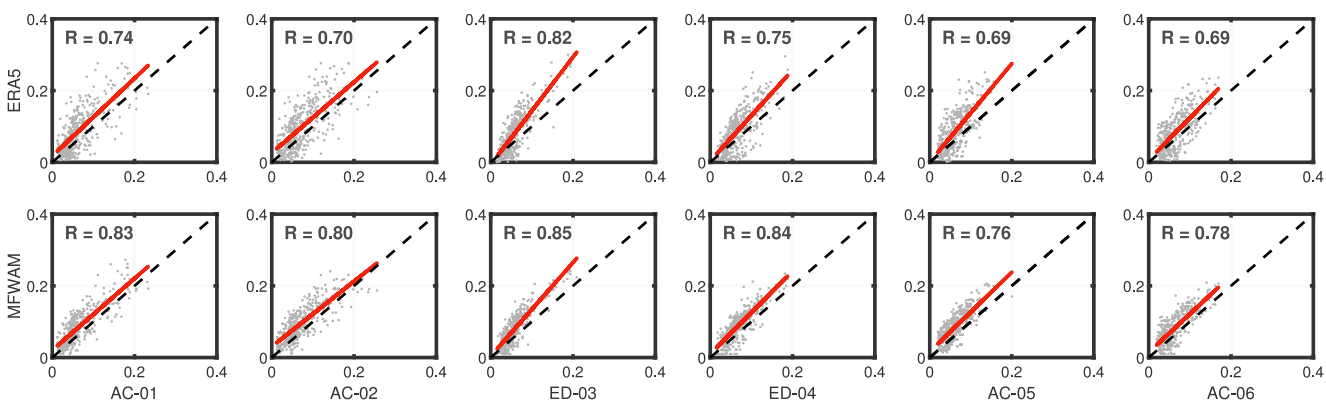


**Figure A1.** Scatter plots of surface Stokes drift versus ERA5 (top panels) and MFWAM (bottom panels) for each drifter separately. A regression line is shown in red color. The dashed black line represents the line of equality when in situ = model. Unit: $\mathrm{m\ s^{-1}}$.

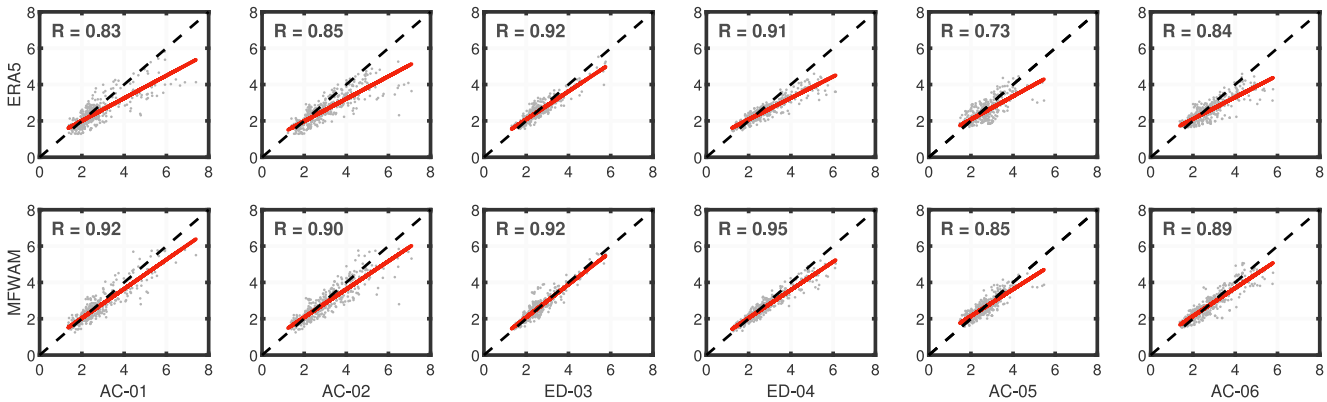


**Figure A2.** Scatter plots of significant wave height from drifters versus ERA5 (top panels) and MFWAM (bottom panels) for each drifter separately. A regression line is shown in red color. The dashed black line represents the line of equality when in situ = model. Unit: m.

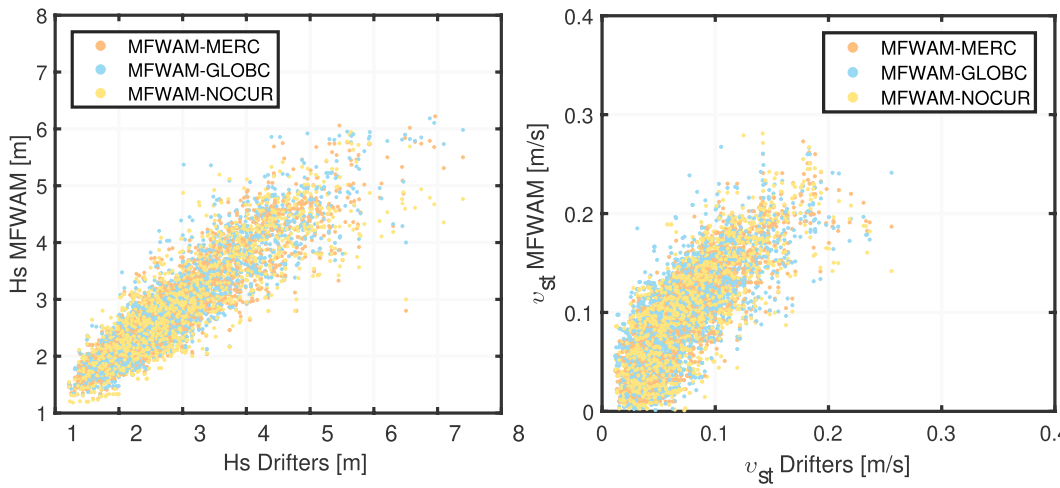


**Figure A3.** Scatter plots of significant wave height (left-panel) and surface Stokes drifts (right-panel) as obtained from the drifters and the customized MFWAM runs.

## Data Availability Statement

Wave model and satellite products supporting the findings of this study are publicly available and can be downloaded from https://doi.org/10.48670/moi-00179 (*Global Ocean L3 Significant Wave Height From NRT Satellite Measurements*), https://doi.org/10.48670/moi-00017 (*MFWAM*), https://doi.org/10.24381/cds.adbb2d47 (*ERA5*), https://doi.org/10.48670/moi-00016 (*Mercator*), and https://doi.org/10.48670/mds-00327 (*Globcurrent*). The drifter measurements collected during the One Ocean Expedition (2021–2023) as well as the customized MFWAM products will be openly available in the 4TU.ResearchData repository of TU Delft (https://data.4tu.nl/).

**Acknowledgments**
The authors would like to thank the European Space Agency (ESA) and the Nansen Environmental and Remote Sensing Center (NERSC) for funding the data collection campaign. Moreover, the authors would like to thank the anonymous reviewers for their valuable comments and feedback. The OpenMetBuoys were built by Gaute Hope (MET Norway) and partly funded by MET Norway.

## References

Altiparmaki, O., Kleinherenbrink, M., Naeije, M., Slobbe, C., & Visser, P. (2022). SAR altimetry data as a new source for swell monitoring. *Geophysical Research Letters*, *49*(7), e2021GL096224. https://doi.org/10.1029/2021GL096224

Aouf, L., Dalphinet, A., Hauser, D., Delaye, L., Tison, C., Chapron, B., et al. (2019). On the assimilation of CFOSAT wave data in the wave model MFWAM: Verification phase. In *IGARSS 2019—2019 IEEE International Geoscience and Remote Sensing Symposium* (pp. 7959–7961). https://doi.org/10.1109/IGARSS.2019.8900180

Ardhuin, F., Marié, L., Rascle, N., Forget, P., & Roland, A. (2009). Observation and estimation of Lagrangian, Stokes, and Eulerian Currents induced by wind and waves at the sea surface. *Journal of Physical Oceanography*, *39*(11), 2820–2838. https://doi.org/10.1175/2009JPO4169.1

Ardhuin, F., Rogers, E., Babanin, A., Filipot, J., Magne, R., Roland, A., et al. (2010). Semiempirical dissipation source functions for ocean waves. Part I: Definition, calibration, and validation. *Journal of Physical Oceanography*, *40*(9), 1917–1941. https://doi.org/10.1175/2010JPO4324.1

Barnes, M. A., & Rautenbach, C. (2020). Toward operational wave-current interactions over the Agulhas current system. *Journal of Geophysical Research: Oceans*, *125*(7), e2020JC016321. https://doi.org/10.1029/2020JC016321

Bohlinger, P., Breivik, Ø., Economou, T., & Müller, M. (2019). A novel approach to computing super observations for probabilistic wave model validation. *Ocean Modelling*, *139*, 101404. https://doi.org/10.1016/j.ocemod.2019.101404

Breivik, Ø., Bidlot, J.-R., & Janssen, P. A. (2016). A Stokes drift approximation based on the Phillips spectrum. *Ocean Modelling*, *100*, 49–56. https://doi.org/10.1016/j.ocemod.2016.01.005

Breivik, Ø., Janssen, P., & Bidlot, J. (2014). Approximate Stokes drift profiles in deep water. *Journal of Physical Oceanography*, *44*(9), 2433–2445. https://doi.org/10.1175/JPO-D-14-0020.1

Clarke, A. J., & Van Gorder, S. (2018). The relationship of near-surface flow, stokes drift and the wind stress. *Journal of Geophysical Research: Oceans*, *123*(7), 4680–4692. https://doi.org/10.1029/2018JC014102

Dalphinet, A., Aouf, L., Law-Chune, S., & Tressol, M. (2023). *Product user manual for global ocean wave analysis and forecasting product* (technical report). EU Copernicus Marine Service. Retrieved from https://catalogue.marine.copernicus.eu/documents/PUM/CMEMS-GLO-PUM-001-027.pdf

Ferry, N., Rémy, E., Brasseur, P., & Maes, C. (2007). The Mercator global ocean operational analysis system: Assessment and validation of an 11-year reanalysis. *Journal of Marine Systems*, *65*(1), 540–560. https://doi.org/10.1016/j.jmarsys.2005.08.004

Halsne, T., Christensen, K. H., Hope, G., & Breivik, Ø. (2023). Ocean wave tracing v.1: A numerical solver of the wave ray equations for ocean waves on variable currents at arbitrary depths. *Geoscientific Model Development*, *16*(22), 6515–6530. https://doi.org/10.5194/gmd-16-6515-2023

Hart-Davis, M. G., Backeberg, B. C., Halo, I., van Sebille, E., & Johannessen, J. A. (2018). Assessing the accuracy of satellite derived ocean currents by comparing observed and virtual buoys in the Greater Agulhas Region. *Remote Sensing of Environment*, *216*, 735–746. https://doi.org/10.1016/j.rse.2018.03.040

Hayne, G. (1980). Radar altimeter mean return waveforms from near-normal-incidence ocean surface scattering. *IEEE Transactions on Antennas and Propagation*, *28*(5), 687–692. https://doi.org/10.1109/TAP.1980.1142398

Hersbach, H., Bell, B., Berrisford, P., Hirahara, S., Horányi, A., Muñoz-Sabater, J., et al. (2020). The ERA5 global reanalysis. *Quarterly Journal of the Royal Meteorological Society*, *146*(730), 1999–2049. https://doi.org/10.1002/qj.3803

Holthuijsen, L. H. (2007). *Waves in oceanic and coastal waters*. Cambridge University Press. https://doi.org/10.1017/CBO9780511618536

Irvine, D. E., & Tilley, D. G. (1988). Ocean wave directional spectra and wave-current interaction in the Agulhas from the shuttle imaging radar-b synthetic aperture radar. *Journal of Geophysical Research*, *93*(C12), 15389–15401. https://doi.org/10.1029/JC093iC12p15389

Janssen, P., Aouf, L., Behrens, A., Korres, G., Cavalieri, L., Christiensen, K., & Breivik, Ø. (2014). *Final report of work-package 1 of 7th framework program mywave project*. European Commission.

Kenyon, K. E. (1969). Stokes drift for random gravity waves. *Journal of Geophysical Research*, *74*(28), 6991–6994. https://doi.org/10.1029/JC074i028p06991

Kleinherenbrink, M., Ehlers, F., Hernández, S., Nouguier, F., Altiparmaki, O., Schlembach, F., & Chapron, B. (2024). Cross-spectral analysis of SAR altimetry waveform tails. *IEEE Transactions on Geoscience and Remote Sensing*, *62*, 1–15. https://doi.org/10.1109/TGRS.2024.3402390

Komijani, H., & Monbaliu, J. (2019). The wave-current interaction in the coastal area. *Journal of Marine Research*, *77*(5), 375–405. Retrieved from https://elischolar.library.yale.edu/journal_of_marine_research/469

Krug, M., Mouche, A., Collard, F., Johannessen, J. A., & Chapron, B. (2010). Mapping the Agulhas current from space: An assessment of ASAR surface current velocities. *Journal of Geophysical Research*, *115*(C10). https://doi.org/10.1029/2009JC006050

Kudryavtsev, V., Yurovskaya, M., Chapron, B., Collard, F., & Donlon, C. (2017). Sun glitter imagery of surface waves. Part 2: Waves transformation on ocean currents. *Journal of Geophysical Research: Oceans*, *122*(2), 1384–1399. https://doi.org/10.1002/2016JC012426

Lellouche, J., Le Galloudec, O., Regnier, C., Van Gennip, S., Law Chune, S., Levier, B., et al. (2023). Mercator quality information document. Retrieved from https://catalogue.marine.copernicus.eu/documents/QUID/CMEMS-GLO-QUID-001-024.pdf

Lutjeharms, J. R. E. (2007). Three decades of research on the greater Agulhas current. *Ocean Science*, *3*(3), 129–147. https://doi.org/10.5194/os-3-129-2007

Marghany, M. (2018). Four-dimensional wave refraction from Sentinel-1A satellite data. *IOP Conference Series: Earth and Environmental Science*, *169*(1), 012030. https://doi.org/10.1088/1755-1315/169/1/012030

Murphy, A. H. (1988). Skill scores based on the mean square error and their relationships to the correlation coefficient. *Monthly Weather Review*, *116*(12), 2417–2424. https://doi.org/10.1175/1520-0493(1988)116<2417:SSBOTM>2.0.CO;2

Naeije, M., Wakker, K., Scharroo, R., & Ambrosius, B. (1992). Observation of mesoscale ocean currents from GEOSAT altimeter data. *ISPRS Journal of Photogrammetry and Remote Sensing*, *47*(5), 347–368. https://doi.org/10.1016/0924-2716(92)90038-B

Pascolo, S., Petti, M., & Bosa, S. (2018). Wave–current interaction: A 2DH model for turbulent jet and bottom-friction dissipation. *Water*, *10*(4), 392. https://doi.org/10.3390/w10040392

Pollard, R. T. (1980). Properties of near-surface inertial oscillations. *Journal of Physical Oceanography*, *10*(3), 385–398. https://doi.org/10.1175/1520-0485(1980)010<0385:PONSIO>2.0.CO;2

Ponce de León, S., & Guedes Soares, C. (2021). Extreme waves in the Agulhas current region inferred from SAR wave spectra and the swan model. *Journal of Marine Science and Engineering*, *9*(2), 153. https://doi.org/10.3390/jmse9020153

Quilfen, Y., & Chapron, B. (2019). Ocean surface wave-current signatures from satellite altimeter measurements. *Geophysical Research Letters*, *46*(1), 253–261. https://doi.org/10.1029/2018GL081029

Quilfen, Y., Yurovskaya, M., Chapron, B., & Ardhuin, F. (2018). Storm waves focusing and steepening in the Agulhas current: Satellite observations and modeling. *Remote Sensing of Environment*, *216*, 561–571. https://doi.org/10.1016/j.rse.2018.07.020

Rabault, J., Müller, M., Voermans, J., Brazhnikov, D., Turnbull, I., Marchenko, A., et al. (2023). A dataset of direct observations of sea ice drift and waves in ice. *Scientific Data*, *10*(1), 251. https://doi.org/10.1038/s41597-023-02160-9

Rabault, J., Nose, T., Hope, G., Müller, M., Breivik, Ø., Voermans, J., et al. (2022). Openmetbuoy-v2021: An easy-to-build, affordable, customizable, open-source instrument for oceanographic measurements of drift and waves in sea ice and the open ocean. *Geosciences*, *12*(3), 110. https://doi.org/10.3390/geosciences12030110

Raney, R. (1998). The delay/Doppler radar altimeter. *IEEE Transactions on Geoscience and Remote Sensing*, *36*(5), 1578–1588. https://doi.org/10.1109/36.718861

Rapizo, H., Durrant, T., & Babanin, A. (2018). An assessment of the impact of surface currents on wave modeling in the southern ocean. *Ocean Dynamics*, *68*(8), 939–955. https://doi.org/10.1007/s10236-018-1171-7

Ren, L., Yang, J., Xiao, Q., Zheng, G., & Wang, J. (2017). On CFOSAT swim wave spectrometer retrieval of ocean waves. In *2017 IEEE International Geoscience and Remote Sensing Symposium (IGARSS)* (pp. 1966–1969). https://doi.org/10.1109/IGARSS.2017.8127365

Rio, M.-H., Mulet, S., & Picot, N. (2014). Beyond GOCE for the ocean circulation estimate: Synergetic use of altimetry, gravimetry, and in situ data provides new insight into geostrophic and Ekman currents. *Geophysical Research Letters*, *41*(24), 8918–8925. https://doi.org/10.1002/2014GL061773

Torres, R., Snoeij, P., Davidson, M., Bibby, D., & Lokas, S. (2012). The Sentinel-1 mission and its application capabilities. In *2012 IEEE International Geoscience and Remote Sensing Symposium* (pp. 1703–1706). https://doi.org/10.1109/IGARSS.2012.6351196